Ribozyme-Catalyzed Aminoacylation from CoA Thioesters†

Na Li and Faqing Huang*

Department of Chemistry and Biochemistry, University of Southern Mississippi, Hattiesburg, Mississippi 39406-5043

Received November 17, 2004; Revised Manuscript Received January 11, 2005

ABSTRACT: Coenzyme A (CoA) thioesters play essential roles in modern metabolism. To demonstrate plausible biochemical functions of thioesters in the RNA world, we have isolated a new class of ribozymes (ACT) that catalyze self-aminoacylation from a number of CoA thioesters with catalytic efficiencies ranging from 7000 to 24 000 $M^{-1}\cdot min^{-1}$. Active thioester substrates are required to contain both a free α-amino group in the acyl moiety and a CoA as the thiol component. We hypothesize ribozyme-based aminoacylation systems using aminoacyl thioesters of CoA as the ancestors of modern aminoacyl tRNA synthetases. On the basis of our previous results [Huang et al. (2000) *Biochemistry 39*, 15548−15555; Coleman and Huang (2002) *Chem. Biol*. *9*, 1227−1236], an extensive RNA-catalyzed "metabolic pathway" involving CoA and its thioesters is proposed. Complex contemporary metabolic systems could have evolved from the proposed ribozyme pathways.

Coenzyme A (CoA)[1] and its thioesters are ubiquitous in all living organisms and play central roles in complex metabolism (*1*). Biologically, thioesters are synthesized by a number of mechanisms, oxidative decarboxylation reactions (such as the formation of acetyl CoA and succinyl CoA from respective pyruvate and α-ketoglutarate), acyl CoA synthetase-catalyzed reactions, *β* oxidation of fatty acids, and catabolism of amino acids. A thioester bond represents an optimal balance between a "high energy" bond and sufficient chemical stability. Therefore, thioesters of CoA are well-suited to participate in a variety of transacylation reactions. These reactions include citric acid synthesis in the citric acid cycle, fatty acid biosynthesis, acylglycerol synthesis, and biosynthesis of amino acids. In addition, polyketide synthases (PKS) and nonribosomal polypeptide synthetases (NRPK) use thioesters of fatty acids and amino acids as the key intermediates to assemble bioactive polyketides and peptides (*2*−*5*).

Extensive biological evidence indicates CoA's ancient origin at least back to the last universal common ancestor of life (*6*). The complex and peculiar structure of CoA further suggests CoA as a molecular vestige (*7*, *8*) from an RNA world (*9*). We have recently demonstrated that RNA (the CoES ribozyme) is indeed capable of CoA synthesis from its precursor phosphopantetheine (*10*). The result provides a possible explanation on the dilemma of CoA's complex universal structure versus its relatively simple sulfhydryl-based biochemical function, as the result of CoA evolutionary history instead of its functional requirement. With plausible prebiotic syntheses of pantoic acid and pantetheine from simpler organic molecules (*11*, *12*) and demonstrated RNA-catalyzed CoA synthesis (*10*), CoA might have played similar biochemical roles in an RNA world to its contemporary biological functions. Subsequent experiments from our laboratory have succeeded in the isolation of a number of RNA sequences (TES ribozymes) that catalyze thioester synthesis on RNA-linked CoA (*13*), providing much needed experimental evidence to support the availability of CoA and its thioesters in the RNA world. Furthermore, the two RNA-catalyzed reactions (CoA and its thioester syntheses) display some salient features of a metabolic pathway of extant biology. The product of the first reaction catalyzed by one ribozyme (CoES) acts as the substrate for a subsequent reaction catalyzed by a different enzyme (TES). Although not yet demonstrated, this proto-type ribozyme-based "metabolic pathway" may also be regulated by its substrates, intermediates, products, and other factors. Because it has been shown that RNA's activities can be modulated by a variety of mechanisms (*14*−*25*), this RNA property should be readily incorporable into the ribozyme pathways to regulate their synthetic activities.

To demonstrate the possible biochemical utility of thioesters and expand the CoA-centered metabolic ribozyme pathway in the context of an RNA era, we have been continuing our pursuit of new ribozymes that involve CoA and its thioesters. Using aminoacyl thioesters of CoA as substrates, we have now isolated a new class of ribozymes that efficiently catalyze self-aminoacylation reactions. The current finding not only adds further experimental evidence to the possible synthesis and utilization of CoA and its thioesters in the RNA world but also suggests the plausible existence of extensive RNA-based metabolic pathways involving CoA and its thioesters in coherently linked multiple reactions.

MATERIALS AND METHODS

Thioester Preparation. An aminoacyl thioester of CoA, BiocytinCoA, was used in the ribozyme selection. Biocyt-

† This work was supported by a NASA Grant NAG5-10668.

* To whom all correspondence should be addressed. Telephone: (601) 266-4371. Fax: (601) 266-6075. E-mail: faqing.h.huang@usm.edu.

[1] Abbreviations: aaRS, aminoacyl tRNA synthetase; BiocytinAMP, biocytinyl adenylate; BiocytinCoA, biocytinyl coenzyme A; BiocytinMPA, biocytinyl mercaptopropionic acid; BiotinAMP, biotinyl adenylate; BiotinCoA, biotinyl CoA.; CoA, coenzyme A; GlyAMP, glycinyl adenylate; GlyCoA, glycinyl CoA; MPA, mercaptopropionic acid; NRPK, nonribosomal polypeptide synthetase; PKS, polyketide synthase; SerAMP, serinyl adenylate; SerCoA, serinyl CoA.

10.1021/bi047576b CCC: $30.25
Published on Web 02/22/2005

inCoA was prepared by imidazole-catalyzed thioesterification (*13*) of CoA using biocytinyl adenylate (BiocytinAMP). Briefly, a mixture of 10 mM BiocytinAMP, 10 mM CoA (Sigma), and 100 mM imidazole (pH 6.5, Sigma) was incubated for 10 min at 25 °C to afford BiocytinCoA. Purification of BiocytinCoA was achieved by reverse-phase HPLC under the following conditions: the BiocytinCoA sample was loaded onto a Delta Pak 7.8 × 300 mm C18 column, which was pre-equilibrated with 100% water. After the column was washed with water for 30 min (5 mL/min), pure BiocytinCoA was eluted with 40% MeOH. The collected solution was concentrated under vacuum and stored at −20 °C. BiocytinAMP was prepared from biocytin (Sigma) and AMP (Sigma) according to the established procedure (*13*, *26*). BiocytinAMP was purified by the same HPLC procedure as for BiocytinCoA purification. The pH of the collected BiocytinAMP solution was adjusted to 3.5 with 1 N HCl and then concentrated under vacuum. It was stored at −80 °C before use. Several other CoA thioesters were synthesized to test substrate specificity of isolated ribozymes. Glycinyl CoA (GlyCoA), serinyl CoA (SerCoA), and biotinyl CoA (BiotinCoA) were synthesized by the same imidazole-catalyzed reaction of CoA with adenylates (GlyAMP, SerAMP, and BiotinAMP). Biocytinyl thioester of mercaptopropionic acid (BiocytinMPA) was similarly prepared by imidazole-catalyzed reaction of BiocytinAMP with mercaptopropionic acid (MPA, Sigma).

Selection Procedure. The starting DNA library was constructed according to published procedures (*10*, *13*). It consisted of a random region of 60 nucleotides flanked by two primer sequences: agtaatacgactcactatt**a**gggaagtgctacc-$\mathbf{N}_{60}$-cgggcatgcggccagcca (bold **a**, initiating nucleotide). About 2×10^{14} different sequences (340 pmol) of the random DNA library were used to generate the initial RNA (∼10 nmol of 92 nt RNA, ∼30 copies per random sequence) pool by T7 *in vitro* transcription. After the reaction of RNA pools with BiocytinCoA, biocytin-tagged RNA was purified by affinity chromatography using Neutravidin (Pierce) resins (*10*, *13*). Neutravidin is a modified version of avidin, resulting in lower nonspecific binding. For the first seven rounds of selection, RNA libraries were incubated with 0.2 mM BiocytinCoA in the selection buffer for 10 min at 25 °C. During the subsequent rounds, selection conditions were changed to lower substrate concentrations and shorter incubations times, 0.1 mM BiocytinCoA and 5 min of incubation for the 8th round, 0.05 mM BiocytinCoA and 2 min of incubation for the 9th and 10th rounds, and 0.01 mM BiocytinCoA and 2 min of incubation for the 11th round. The selection buffer consisted of 20 mM HEPES (pH 7.4), 200 mM KCl, 100 mM NaCl, 30 mM $MgCl_2$, and 10 mM $CaCl_2$. After incubation, free BiocytinCoA was removed by membrane filtration (Microcon-30, Millipore). Recovered RNA from Neutravidin-affinity chromatography was reverse-transcribed and PCR-amplified to generate DNA templates for the next round of selection. After 11 rounds of selection, the resulting DNA pool was cloned and sequenced by the standard procedure (*27*).

Reaction-Site Mapping. Reaction sites on isolated ribozymes were mapped by primer extension reactions (*28*). Substrate-reacted RNA (1 μM in 10 μL of solution) was mixed with 1 mM each of dNTP and 1 μM 5′-^{32}P-labeled reverse primer. The mixture was heated at 85 °C for 1 min and then allowed to cool to 25 °C. A total of 2 μL of 5× RT buffer (250 mM Tris at pH 8.3, 250 mM KCl, 50 mM $MgCl_2$, and 2 mM DTT) and 10 units of AMV reverse transcriptase were added to the reaction solution, and the sample was incubated for 30 min at 42 °C. The resulting ^{32}P-labeled cDNA fragments were fractionated by 8% denaturing PAGE (40 × 35 cm) and visualized by phosphorimaging.

Reaction Product Identification. Aminoacylation products from isolated RNA sequences were analyzed first by HPLC after nuclease P1 (Pharmacia) digestion of substrate-reacted RNA, followed by mass spectrometry (MS) analysis. Both unreacted and substrate-reacted RNA was separately incubated with 1 unit of nuclease P1 for 5 min at 25 °C in the nuclease P1 buffer (10 mM NaAc and 0.4 mM $ZnCl_2$ at pH 5.2). The digests were individually loaded onto a C18 column (Alltech Econosphere, 4.6 × 50 mm), eluting with 15% MeOH and 85% water at a flow rate of 0.8 mL/min. The collected aminoacylation products from HPLC were vacuum-dried and then analyzed by MALDI−TOF MS (Macromolecular Resources, Fort Collins, CO).

Kinetic Analysis. Ribozyme-catalyzed aminoacylation rates of three RNA sequences (ACT1, ACT3, and ACT6) (named after aminoacylation from CoA thioester) were determined under different substrate concentrations. Internally ^{32}P-labeled RNA was incubated with various concentrations of BiocytinCoA in the selection buffer at 25 °C. Aliquots were withdrawn at varying time points, quenched by adding 50 mM EDTA, and then ethanol-precipitated. Recovered RNA was incubated with 1 μg of streptavidin. Biotinylated RNA−streptavidin complexes were then easily separated from unreacted RNA by PAGE (10−20 min of running time to minimize potential hydrolysis of aminoacylated RNA) and quantitated by phosphorimaging. Pseudo-first-order reaction rate constants (k_{ob}) were derived from fitting the product yield−reaction time data to the first-order kinetic equation. The resulting k_{ob}−[substrate] data sets were then fitted (*10*, *13*) to the Michaelis−Menten equation to obtain kinetic parameters k_{cat} and K_M. Lineweaver−Burk double-reciprocal plots of the same data sets gave similar results within the error limits. Under each substrate concentration, the reaction rate was determined in either duplicate or triplicate on different days to assess the variations of the kinetic experiments, which are reported as the errors of the kinetic parameters k_{cat} and K_M in Figure 5.

Substrate Specificity. Internally ^{32}P-labeled ACT3 ribozyme was incubated separately with 1 mM of various thioesters including BiocytinCoA, BiocytinMPA, GlyCoA, SerCoA, and BiotinCoA in the selection buffer for 2 h at 25 °C. Reactions were quenched by adding gel-loading buffer containing 50 mM EDTA. Because of the potential hydrolysis of aminoacylated RNA (*29*, *30*) during long gel electrophoresis in the TBE buffer, reacted RNA was fractionated from unreacted RNA by acid polyacrylamide gel electrophoresis (*31*). Aminoacylated RNA is fairly stable under acidic conditions.

Ribozyme 3′ and 5′ Boundaries. To determine the 3′ boundary of active ACT3, RNA was 5′-end-labeled by ^{32}P through [γ-^{32}P]ATP-initiated transcription (including [γ-^{32}P]-ATP in the transcription solution). The resulting 5′-labeled RNA was partially hydrolyzed (5 min at 90 °C in 50 mM $NaHCO_3$, with 1 μg of tRNA added as a carrier) to generate

Scheme 1: Selection Scheme for Isolation of Ribozymes Capable of Self-Aminoacylation from Biocytinyl Thioester of CoA (BiocytinCoA)

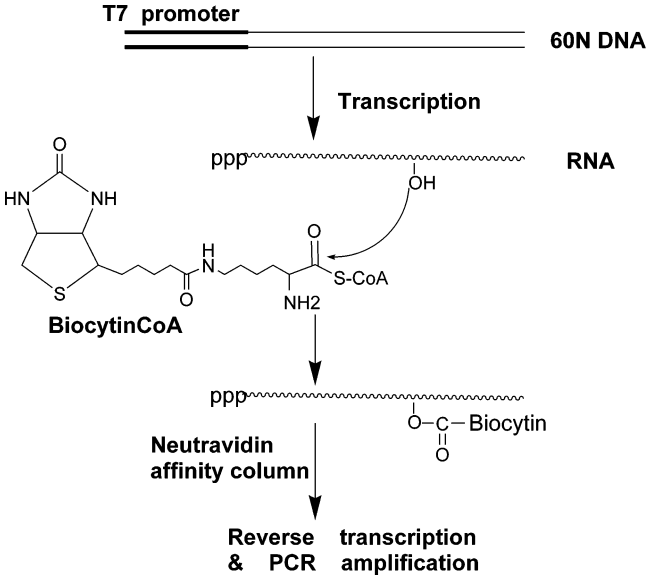

RNA fragments, which were EtOH-precipitated. A small portion of the recovered RNA fragments was saved to serve as an RNA fragment ladder. The rest was reacted with 1 mM BiocytinCoA for 10 min at 25 °C. Active RNA fragments would be tagged by biocytin, allowing their isolation by Neutravidin-affinity chromatography. Recovered RNA fragments from the column were fractionated by 8% PAGE along with the RNA fragment ladder and a ^{32}P-labeled 55-nt DNA marker.

The active 5′ boundary of ACT3 was determined by primer extension (*28*). Unlabeled ACT3 RNA was partially digested under the same conditions as described above. RNA fragments were then reacted with 1 mM BiocytinCoA for 10 min. Reacted RNA fragments were purified by Neutravidin chromatography. Recovered RNA fragments from the column were used as templates for reverse transcription under the same conditions as described in Reaction-Site Mapping. ^{32}P-labeled cDNA was analyzed by PAGE.

Construction of Smaller Ribozymes. On the basis of the above boundary experiments and computer-predicted RNA secondary structure (*32*) (Figure 7C), two shorter versions of ACT3 were constructed by transcription of shortened DNA templates. ACT3-tr1 corresponds to the original ACT3 sequence of 1−57, and ACT3-tr2 is a further modified sequence of ACT3-tr1, with the top stem-loop (31−45) removed.

RESULTS

Selection of Ribozymes with Aminoacylation Activity. From previous results of optimal random RNA size and catalytic activity relationship (*10*, *13*), an RNA library with a 60N random region was used for the isolation of ribozymes with aminoacylation activities from aminoacyl CoA. The selection scheme is shown in Scheme 1. A total of 11 rounds of selection−amplification cycles were performed under different reaction conditions (Figure 1). Selection yields, measured by RNA retained on the Neutravidin column over total RNA, were used to monitor the selection progress. As can be seen from Figure 1, there was no change in the

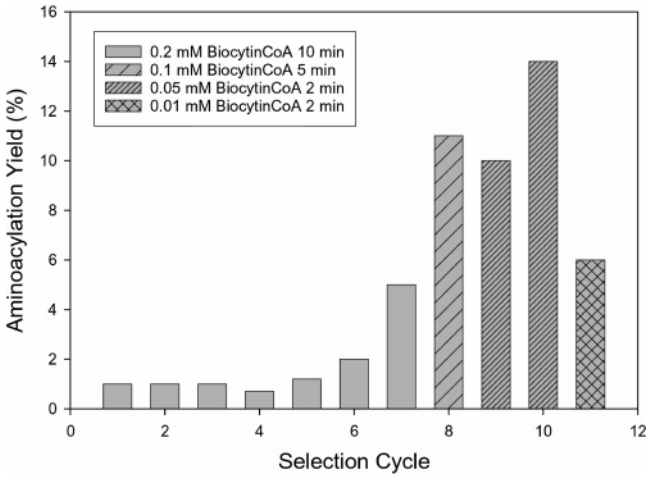

FIGURE 1: Pool biotin-tagged RNA yields versus selection cycle. More stringent conditions (lower substrate concentrations and shorter incubation times) were applied in later rounds of selection. The 2-fold decrease in RNA yields in the last round before cloning was due to a 5-fold reduction on the substrate concentration.

background during the first five rounds of selection. From the sixth round, isolated RNA yields started to rise. During the last four rounds of selection, reaction conditions were changed (lower substrate concentrations and shorter reaction times) to isolate more efficient ribozymes. The last round had lower RNA yields than the previous three rounds because of a much lower substrate concentration (10 μM). The DNA pool from the 11th round was then cloned and sequenced.

Isolated RNA Sequences. A total of 26 clones were obtained. Most *in vitro* selections yield multiple families of heterogeneous RNA sequences (*10*, *13*, *33*, *34*). However, the current selection produced only a single RNA family (Figure 2). Similar results were obtained from other laboratories for the selection of ribozymes that catalyze amino acid transfer reactions (*35*−*37*). All of the isolated clones can be assigned to three representative sequences, ACT1, ACT3, and ACT6, with a high degree of sequence homology. The other three sequences were derived from ACT1 and ACT3 by point mutations. While ACT1 and ACT6 are each 59 nt in the original random region (60N), surprisingly, ACT3 has only 46 nt in the same region. Furthermore, ACT3 has the exact same sequence as the random region 14−59 of ACT1. The probability of two independent sequences having the same 46-nt sequence is $^1/_4{}^{46} = 2 \times 10^{-28}$. Because the number of different sequences in the starting RNA library was 2×10^{14}, it was very unlikely (a probability of 4×10^{-14}) that ACT1 and ACT3 originated from different sequences, even if the original random RNA library had contained the same RNA sizes as that of ACT3. In other word, ACT3 was almost certainly derived from ACT1 by shortening 13 nt through an unknown mechanism. Yet, ACT3 and its two mutants ACT4 and ACT5 dominated the final selection pool ($^{22}/_{26} = 85\%$). Preliminary experiments (cycles of PCR, transcription, and reverse transcription) with ACT1 designed to provide an explanation for the origin of ACT3 have not yielded constructive information.

Reaction-Site Mapping. Reaction sites on the three representative ACT1, ACT3, and ACT6 were mapped by reverse-transcriptase-catalyzed primer extension reactions. Unless the reaction sites were within the reverse primer region or at/near the 5′ end, the 2′-modified RNA sites would

Clone	Sequence	Repeats
ACT1	GUCACAAUCGACCAAAGCACCAUGAAGGGGACCUAUCCUGGGUCCAGUUCAAUCCCUGC	1
ACT2	GUCACAAUCGACCAAAGCACCAUGAAGGGGGCCUAUCCUGGGCCCAGUUCAAUCCCUGC	1
ACT3	AAAGCACCAUGAAGGGGACCUAUCCUGGGUCCAGUUCAAUCCCUGC	20
ACT4	AAAGCACCAUGAAGGGGACCUAUCCUGGGUCCAGUUCAAUCCCUGA	1
ACT5	AAAGCACCAUGAAGGGGACCUAUCCUGGGUCCAGUUCAAUCCUUGC	1
ACT6	AAAGCACC AGGGG CCGAUAAUCGG CCAGUUUAAUCCCACACCGCAGUGCUCCGA	2
	G U	
	U U A	

FIGURE 2: Aligned RNA sequences from isolated 26 clones. Only the sequence portions derived from the original 60N random region are shown. The full RNA sequences can be constructed by adding two primer sequences, agggaagugcuacc to the 5′ end and cgggcaugcggccagcca to the 3′ end of the sequences in the figure. Conserved nucleotides are underlined. The same reactive uridine (U) site is in bold.

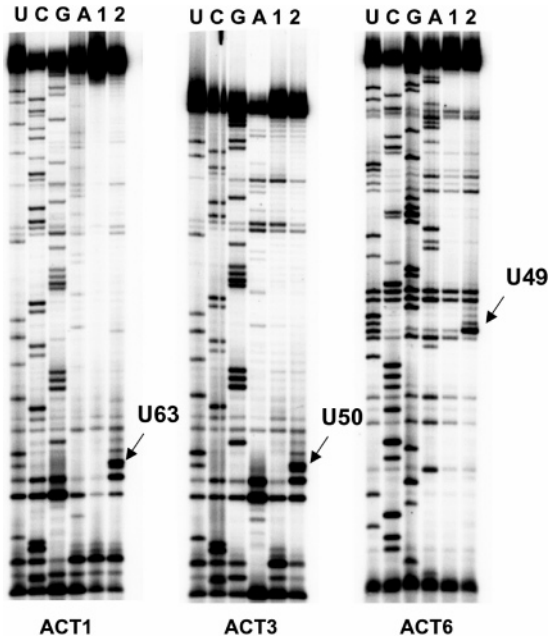

FIGURE 3: RNA reaction-site mapping by reverse-transcriptase-catalyzed primer extension with the ^{32}P-labeled reverse primer, followed by 8% PAGE analysis. RNA sequencing lanes by the Sanger dideoxy method are labeled as U, C, G, and A. cDNAs from unreacted RNA and BiocytinCoA-reacted RNA are marked as lanes 1 and 2. For each of the three ribozymes (ACT1, ACT3, and ACT6), there is a strong pause site (lane 2) over the background (lane 1), indicating a specific 2′-OH modification by biocytin. All pauses correspond to the same U site after sequence alignment (Figure 2), but they are numbered as U63, U50, and U49 from the 5′ ends of ACT1, ACT3, and ACT6, respectively.

cause reverse-transcription pauses (*28*), which could be determined by PAGE. Figure 3 shows primer extension of unreacted RNA (lane 5) and BiocytinCoA-reacted RNA (lane 6), along with RNA sequencing (lanes 1−4) by the Sanger dideoxy method (*38*). Both ACT1 and ACT3 show strong pauses at the same 29 U from the 3′ ends (but U63 of ACT1 and U50 of ACT3 from the 5′ ends). ACT6 also shows a strong pause at a U site (U49). All of the reactive U sites are located at the same position after sequence alignment. These reaction U sites are marked bold in Figure 2.

Aminoacylation Product Identification. Unreacted and BiocytinCoA-reacted RNAs were separately digested by nuclease P1 and then analyzed by HPLC. Compared with unreacted ACT1 digest, the digest from BiocytinCoA-reacted ACT1 displayed an additional peak at 4.6 min (Figure 4A). Its UV spectrum obtained by the online photodiode array detector is similar to the sum of the spectra of uridine and cytidine (Figure 4B). MS analysis (MOLDI−TOF, low resolution) gave a nice molecular peak at 983.2 (*m*/*z*) for the negative ion (Figure 4C), in good agreement with the predicted molecular weight of a dimer product, pU(Biocytin)-pC (inset of Figure 4C), $C_{34}H_{51}N_9O_{19}P_2S$, MW 983.2. HPLC and MS analyses of ACT3 yielded identical results (not shown) with those of ACT1. Similar HPLC and MS analyses on ACT6 gave a slightly different HPLC retention time (4.8 min, not shown), whose UV spectrum (not shown) resembles that of uridine. A molecular ion at 984.3 (1 unit different from that of ACT1 digest, not shown) was found by MS, again in good agreement with the predicted molecular weight of a dimer product, pU(Biocytin)pU, $C_{34}H_{50}N_8O_{20}P_2S$, MW 984.2. The results indicate that the phosphodiester bond at the 2′ biocytin-modified RNA site is resistant to nuclease P1 digestion. The combined evidence from HPLC, UV absorbance, and MS confirmed the same reaction site (the bold U in Figure 2) as mapped by the reverse-transcriptase-catalyzed primer extension reaction for all isolated ribozyme sequences.

Catalytic Efficiency. Kinetic analysis was performed with the three representative ACT1, ACT3, and ACT6 ribozymes. Figure 5A illustrates the reaction yield−time courses at different substrate concentrations. The pseudo-first-order rate constant (k_{ob}) at different BiocytinCoA concentrations was obtained by nonlinear fitting (*10*, *13*). The resulting k_{ob}−[BiocytinCoA] data were then fitted (Figure 5B) to the Michaelis−Menten equation to obtain k_{cat} and K_M (*10*, *13*). These ribozyme parameters are listed in Figure 5C. All ribozymes display a k_{cat} around 1 min^{-1} with good substrate binding affinities (50−110 μM). ACT3, derived (by shortening 13 nt) from ACT1, is about twice as efficient as ACT1. The kinetic parameters of ACT1 and ACT3 may therefore explain their relative population in the final cloning pool (but not the origin of ACT3). By ribozyme standards, all isolated RNA sequences are relatively efficient ribozymes, with k_{cat}/K_M ranging from 7000 to 24 000 M^{-1}·min^{-1}.

Substrate Specificity. To assess substrate specificity of isolated ribozymes, a series of different thioesters were chemically synthesized and used to react with ACT3 ribozyme. Reacted RNAs were fractionated from unreacted RNA by acid gel electrophoresis (*31*). Figure 6 indicates that BiocytinCoA, GlyCoA, and SerCoA are good substrates for the ribozyme. However, neither BiocytinMPA nor BiotinCoA is able to react with ACT3. Accordingly, the presence of CoA in the thioester substrate is required for the ACT ribozyme activities. Although the acyl group in the CoA thioester may vary, it needs to have a free α-amino group. An α-aminoacyl CoA thioester is therefore a general substrate for the ACT ribozymes.

Ribozyme 3′ and 5′ Boundaries. Both the 3′ and 5′ boundaries of ACT3 ribozyme were determined using

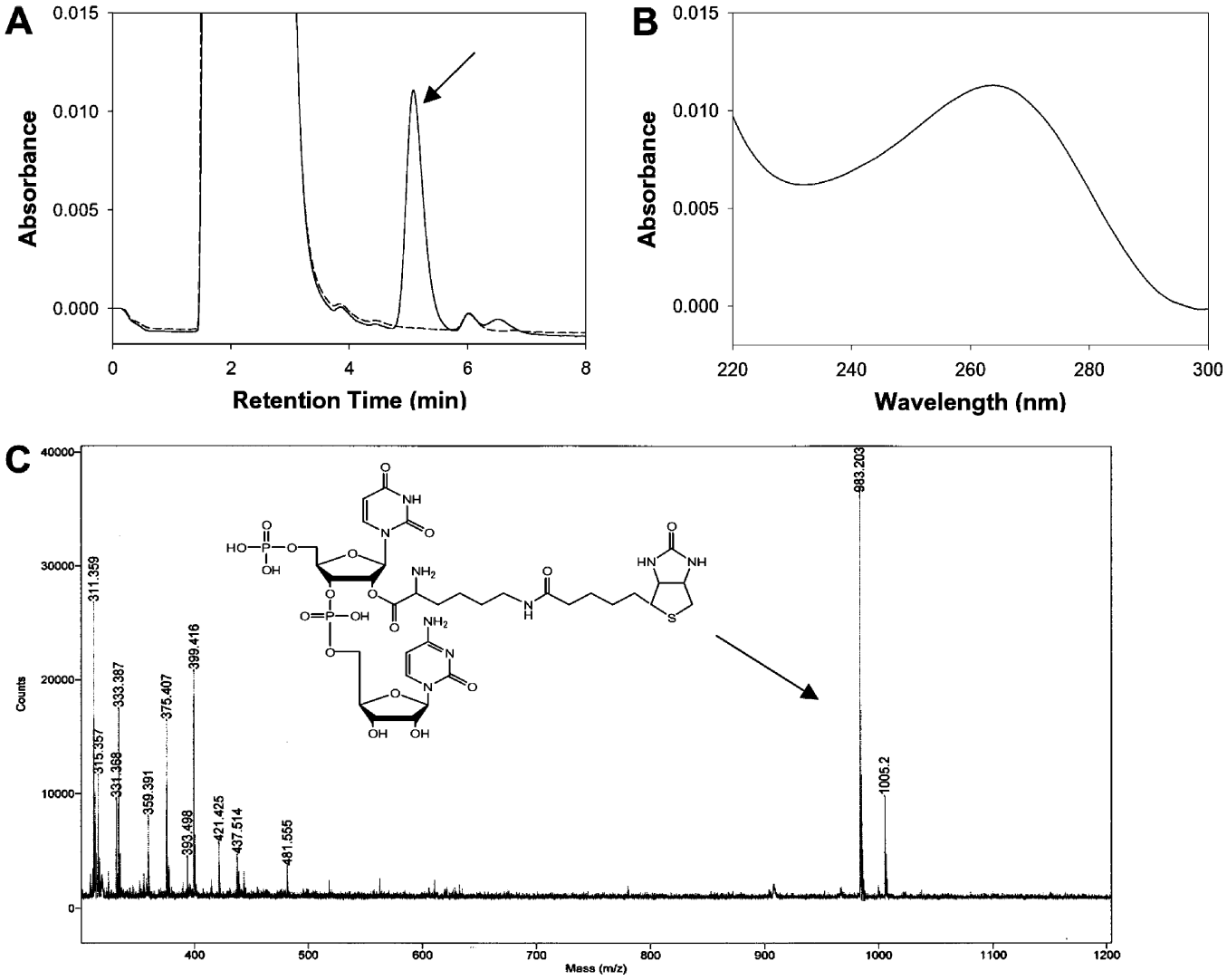

FIGURE 4: RNA aminoacylation product identification (ACT3) by nuclease P1 digestion followed by HPLC, UV, and MS. (A) HPLC analysis of nuclease P1-digested unreacted RNA (···) and BiocytinCoA-reacted RNA (—). The product peak is indicated by an arrow. (B) UV spectrum of the product peak measured by an online photodiode array detector. The spectrum resembles the sum of cytidine and uridine spectra. (C) MS analysis of the product peak from A, confirming the structure (inset) of a biocytin-containing dimer, pU(Biocytin)-pC with a molecular weight of 983.2.

partially hydrolyzed RNA fragments. For 3′-boundary mapping, 5′-^{32}P-labeled RNA (prepared by [γ-^{32}P]ATP initiated transcription) was used. After partial hydrolysis and reaction with BiocytinCoA, reacted RNA fragments were isolated by Neutravidin-affinity chromatography and analyzed by PAGE (Figure 7A). There was clearly a 3′ boundary at C57 for the ribozyme activity. However, there was no detectable 5′ boundary as determined by reverse transcription (Figure 7B). From the computer-predicted secondary structure of ACT3 (Figure 7C), the 3′ boundary at C57 indicates that the 3′ hairpin (formed mostly by the 3′ primer sequence) is not necessary for ribozyme activity. Further shortening from C57 leads to the loss of activity. Because the essential nucleotides U54−C57 near the 3′ boundary are base-paired with the nucleotides g2-a4 at the 5′ end, it is not surprising that the 5′ boundary is the 5′ end of the isolated ribozyme. To confirm the 3′ boundary, a 3′-truncated version of ACT3, ACT3-tr1 (corresponding to 1−57 nt of ACT3), is indeed active (lane 4 of Figure 8). Moreover, ACT3 and ACT3-tr1 display the same enzymatic properties, confirming the nonessential 58−78 nucleotides in ACT3. Further modification of ACT3 by removing the top hairpin results in a total loss of activity (lane 6 of Figure 8), indicating the importance of this hairpin structure for enzymatic function.

DISCUSSION

Expanding our previous work on ribozymes that catalyze the synthesis of CoA (*10*) and its thioesters (*13*), we have performed a relatively straightforward *in vitro* selection experiment (Scheme 1), from which a single family of ACT ribozymes has been isolated from a 60N random RNA library. Using aminoacyl thioesters of CoA as substrates, all of the isolated ACT ribozymes catalyze self-aminoacylation with relatively high efficiencies (k_{cat}/K_M from 7000 to 24 000 $M^{-1}\cdot min^{-1}$ at 25 °C) at the same specific uridine site (after sequence alignment) within the original 60N random region (Figure 2). The ACT ribozymes can accept a broad spectrum of thioester substrates but require both CoA as the thio component and a free α-amino group in the acyl portion. Therefore, a general class of amino acid thioesters of CoA with the formula of R-CH(NH_2)C(O)-S-CoA (R = amino

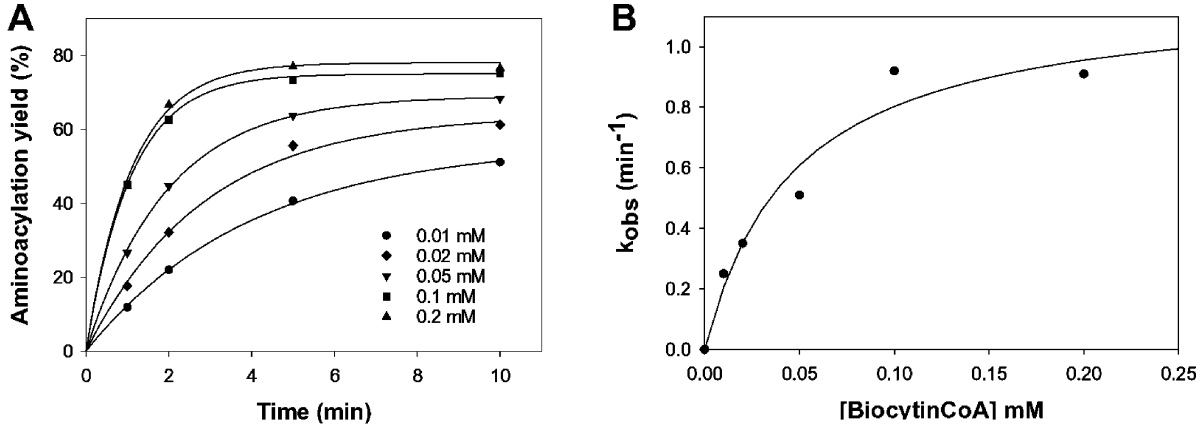

C

Ribozyme	k_{cat} (min^{-1})	K_M (mM)	k_{cat}/K_M ($M^{-1}.min^{-1}$)
ACT1	0.86 ± 0.20	0.08 ± 0.04	11,000 ± 550
ACT3	1.18 ± 0.15	0.05 ± 0.02	24,000 ± 420
ACT6	0.79 ± 0.14	0.11 ± 0.04	7,100 ± 390

FIGURE 5: Kinetic analysis of ACT1, ACT3, and ACT6. (A) ACT3 aminoacylation yields versus reaction time under various substrate concentrations. Rate constants were obtained by fitting the data to a pseudo-first-order kinetic equation. (B) Determination of K_M and k_{cat} by curve-fitting to the Michaelis−Menton equation. (C) Kinetic parameters of ACT1, ACT3, and ACT6 in the selection buffer (pH 7.4) and 25 °C.

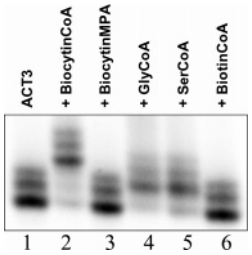

FIGURE 6: Determination of ribozyme substrate specificity. Different substrates (indicated at the top, 1 mM) were incubated with ACT3 for 2 h in the selection buffer at 25 °C. Reaction products were analyzed by acid gel electrophoresis to avoid potential hydrolysis. All aminoacyl thioesters of CoA are active substrates, but other forms of thioesters (missing a free amino group or CoA) are unable to react with ACT3.

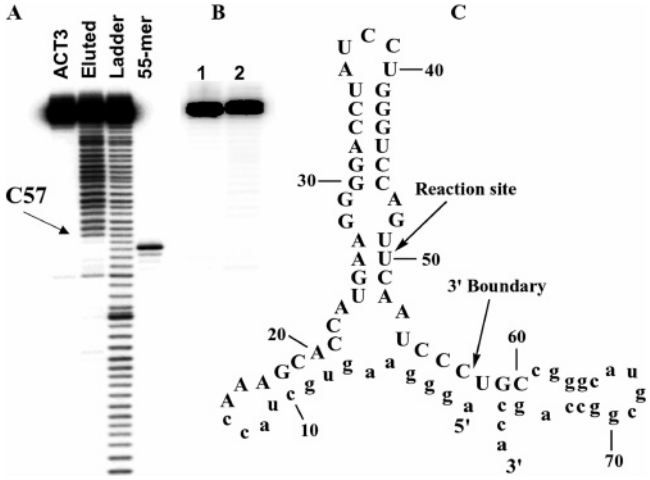

FIGURE 7: ACT3 active boundary determination. (A) 3′-Boundary mapping by reacting of partially hydrolyzed ACT3 (^{32}P labeled) with BiocytinCoA followed by Neutravidin-affinity chromatography. Recovered RNA fragments from the column were then analyzed by PAGE (lane 2), along with unreacted ACT3 (lane 1), a partially hydrolyzed ACT3 ladder (lane 3), and a 55-nt DNA size marker (lane 4). C57 is the 3′ ribozyme active boundary. (B) 5′-Boundary determination by reacting of partially hydrolyzed unlabeled ACT3 with BiocytinCoA followed by Neutravidin-affinity chromatography. Recovered RNA fragments from the column were used as templates for cDNA synthesis using the ^{32}P-labeled reverse primer and then analyzed by PAGE (lane 2), along with cDNA synthesized from unreacted ACT3 (lane 1). No defined 5′ boundary is apparent. (C) Computer-predicted secondary structure of ACT3 by mfold (*32*). The mapped boundaries indicate the unnecessary step loop at the 3′ end for ACT3 activities.

acid side chain) can serve as substrates for the ACT ribozymes.

Because aminoacylation of tRNAs (or tRNA charging by amino acids) by aminoacyl tRNA synthetases (aaRS) is the first essential biochemical step during protein biosynthesis, aminoacylation of RNAs by ancestral ribozymes has been suggested (*37*, *39*−*43*) as a crucial reaction during the transition between an RNA world and the emergence of protein. There has been sustained interest in identifying ribozymes that perform similar aminoacylation reactions as catalyzed by aaRS. The Yarus laboratory has isolated and subsequently engineered a number of efficient ribozymes that self-aminoacylate at their 3′ ends using aminoacyl adenylates (*31*, *41*, *43*−*45*). The catalytic efficiencies of these isolated and engineered ribozymes range from 200 to 60 000 $M^{-1}\cdot min^{-1}$ at 0 °C. An exceptional ribozyme (RNA 77) catalyzes a self-aminoacylation reaction at a k_{cat} of 430 min^{-1} with high substrate specificity for Phe and Tyr (*43*). While attempting to isolate ribozymes for peptide-bond formation, Jenne and Famulok isolated instead ribozymes that performs a transesterification reaction between the substrate Bio-Phe-AMP (an AMP aminoacyl ester) and an RNA internal 2′ OH within the 3′ primer region (*46*). The clone 11 ribozyme has a k_{cat}/K_M of 350 $M^{-1}\cdot min^{-1}$. Lohse and Szostak isolated a ribozyme that is able to transfer a biotinylated methionyl (Biotin-Met) group from the 3′ end of a substrate hexanucleotide to the 5′ OH or -NH_2 of RNA (*35*). The catalytic efficiency of the ribozyme is 12 000 $M^{-1}\cdot min^{-1}$, but a major contribution is from the low K_M value (120 nM) because of the high binding affinity of the hexanucleotide substrate to

Scheme 2: Proposed CoA-Centered Metabolic Pathway in the RNA World[a]

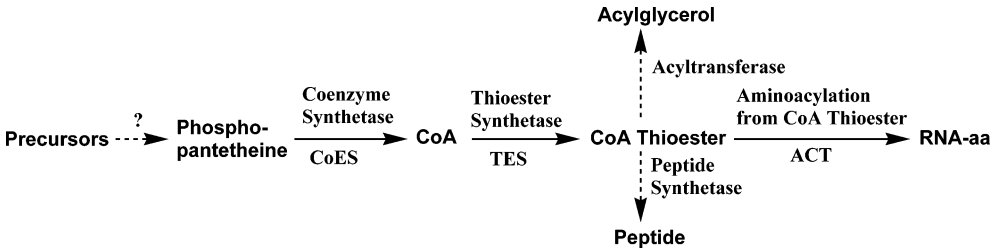

[a] Solid arrows represent demonstrated reactions by ribozyme catalysis from our laboratory, and dotted arrows indicate possible reactions whose ribozyme activities are yet to be discovered.

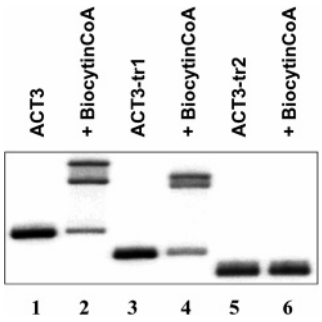

FIGURE 8: Aminoacylation activities of truncated forms of ACT3. ACT3-tr1 has the original 1−57 nucleotides of ACT3. Removal of the top stem loop (31−45) of ACT3-tr1 results in ACT3-tr2. RNAs were incubated with 1 mM BiocytinCoA in the selection buffer for 10 min at 25 °C, and the products were analyzed by the streptavidin gel-shift assay. ACT3-tr1 is clearly active, confirming the boundary experiments (Figure 7). However, further truncation of the top stem loop lead to the complete loss of activities. The double product bands in lanes 2 and 4 are due to RNA dimer−streptavidin formation (*13*).

the ribozyme (*36*). Using biotinylated amino acid cyanomethyl esters (biotin-aa-CME) as substrates, the Suga laboratory has succeeded in isolating a number of ribozymes capable of both cis- and trans-aminoacylation at either the 5′ end (*47*, *48*) or 3′ end (*37*, *49*, *50*) of RNA, with k_{cat}/K_M values from 40 to 1300 $M^{-1}\cdot min^{-1}$. Unlike the other aminoacylating ribozymes, the Suga ribozymes are capable of recognizing tRNAs and catalyzing multiple-turnover aminoacylation reactions on a 3′ hydroxyl group of tRNAs (*37*, *49*, *50*). Except for using different substrates, the ribozymes catalyze the same reactions as the second reaction (aminoacyl transfer) by aaRS. Therefore, the Suga ribozymes represent a significant step toward construction of ribozyme-based aaRS systems.

Differing from all of the previous work on ribozyme-catalyzed RNA aminoacylation (*35*, *37*, *41*, *46*, *47*, *50*), our current selection of aminoacylating ribozymes uses aminoacyl thioesters of CoA as substrates. Our choice of substrates is based on (1) the roles of (amino)acyl thioesters in the synthesis of bioactive polyketides and nonribosomal peptides (*2*−*5*) and (2) our previous demonstration of RNA-catalyzed CoA thioester synthesis from acyl adenylates (*13*), which suggests the availability of CoA thioesters in the RNA world. In addition to acyl adenylates, other unidentified substrates may also be used to synthesize CoA thioester by ribozymes. Furthermore, thioesters of CoA could have also been made available through abiotic chemical processes in the "thioester world" (*51*). Both mechanisms of thioester synthesis could have operated in the RNA world. While aminoacyl adenylates are the natural substrates for the second reaction during aaRS-catalyzed tRNA charging, aminoacyl thioesters of CoA may offer a distinctive advantage, the hydrolytic stability, over aminoacyl adenylates in the context of an RNA world. Because of their hydrolytic libilities, aminoacyl adenylates have very short half-lives [$t_{1/2} \sim 3$ min at pH 7.4 and 25 °C for BiocytinAMP, our measured stability, consistent with reported stability of other aminoacyl adenylates (*52*)]. In fact, newly synthesized aminoacyl adenylates from amino acids and ATP by aaRS are not released into solution but rather used directly for aminoacylation of tRNA by the same aaRS. In stark contrast, aminoacyl thioesters of CoA are relatively stable ($t_{1/2} \sim 6$ h at pH 7.4 and 25 °C for BiocytinCoA, our measured stability). Therefore, aminoacyl thioesters of CoA would have been much better choices as free substrates than aminoacyl adenylates for acyl transfer reactions in the RNA world.

Jakubowski hypothesized that aaRS's were evolved from a noncoded thioester-dependent peptide synthesis system (*53*). On the basis of our previous (*10*, *13*) and current findings and the hydrolytic stability difference between aminoacyl adenylates and aminoacyl thioesters, we further suggest aminoacyl thioesters of CoA as the general acylating substrates for RNA aminoacylation and for peptide synthesis in the RNA world. The contemporary aaRS-based tRNA aminoacylation systems could have originated from the ribozyme-based systems. Three lines of evidence from extant biology support this hypothesis. First, although modern aaRS's do not involve CoA in performing their biochemical functions, many aaRS's retain a separate thiol binding site. If CoA is supplied to a system containing aaRS, amino acids, and ATP, aminoacyl thioesters of CoA are synthesized (*53*, *54*). Whereas some aaRS's use the thiol-binding site for homocysteine editing to form homocycteine thiolactone (*55*, *56*), a thiol-binding site is also present in other aaRS's that apparently do not perform such homocysteine editing (*56*). This nonfunctional thiol-binding site within aaRS could therefore have been a molecular vestige from ancestral RNA enzymes that had possessed aminoacyl thioester-binding sites for using aminoacyl thioesters of CoA as acylating substrates. Second, acyl carrier proteins use a phosphopantetheine prosthetic group to attach an acyl intermediate for acyl transfer, although protein should be capable of forming an acyl thioester on a much simpler cysteine residue. Therefore, acyl carrier proteins might reflect the plausibility of their ancestral ribozymes using acyl CoA. The third supporting evidence comes from the existence of contemporary PKS and NRPK systems that use protein-linked phosphopantetheine thioesters of fatty acids and amino acids as the active intermediates for the synthesis of bioactive polyketides and peptides (*2*−*5*). Both PKS and NRPK systems have the

essential thioester synthesis and acyl transfer functionalities, which could have evolved from ancestral ribozymes. These PKS and NRPK systems have been proposed to have evolved from ancestral ribozyme systems (*53*).

Combining with our previous results on RNA-catalyzed CoA synthesis (*10*) and thioester synthesis (*13*), we propose a ribozyme-based "metabolic pathway" (Scheme 2) that involves CoA and its thioesters as the intermediate metabolites for "biosynthesis" of aminoacyl RNA (RNA-aa, the precursor to tRNA-aa), peptide (the precursor to nonribosomal peptide), and acylglycerol (the ancestral lipid to modern triacylglycerol). Each reaction step may be modulated by substrates, metabolites, and other cofactors to regulate the synthesis of end products.

Although the synthesis of phosphopantetheine by RNA has yet to be identified, plausible prebiotic syntheses of pantoic acid and pantetheine have been demonstrated (*11*, *12*). Consequently, phosphopantetheine could have been synthesized either by prebiotic chemistry, RNA catalysis, or both mechanisms. In addition, more ribozyme-catalyzed chemical steps may be added to Scheme 2 to form an extensive CoA-centered pathway. Therefore, elaborate metabolic systems, the hallmark of contemporary biology, could have developed in the RNA world.

ACKNOWLEDGMENT

We thank the members of our laboratory for comments on a draft manuscript.

REFERENCES

1. Kanehisa, M., Goto, S., Kawashima, S., and Nakaya, A. (2002) The KEGG databases at GenomeNet, *Nucleic Acids Res. 30*, 42−46.
2. Stindl, A., and Keller, U. (1993) The initiation of peptide formation in the biosynthesis of actinomycin, *J. Biol. Chem. 268*, 10612−10620.
3. Dittmann, J., Wenger, R. M., Kleinkauf, H., and Lawen, A. (1994) Mechanism of cyclosporin A biosynthesis. Evidence for synthesis via a single linear undecapeptide precursor, *J. Biol. Chem. 269*, 2841−2846.
4. Stachelhaus, T., Huser, A., and Marahiel, M. A. (1996) Biochemical characterizaiton of peptidyl carrier protein (PCP), the thiolation domain of multifunctional peptide synthetases, *Chem. Biol. 3*, 913−921.
5. Cane, D. E., and Walsh, C. T. (1999) The parallel and convergent universes of polyketide synthases and nonribosomal peptide synthetases, *Chem. Biol. 6*, R319−R325.
6. Benner, S. A., Ellington, A. D., and Tauer, A. (1989) Modern metabolism as a palimpsest of the RNA world, *Proc. Natl. Acad. Sci. U.S.A. 86*, 7054−7058.
7. White, H. B. (1976) Coenzymes as fossils of an earlier metabolic state, *J. Mol. Evol. 7*, 101−104.
8. White, H. B. (1982) in *The Pyridine Nucleotide Coenzymes* (Everse, J., Anderson, B., and Yu, K.-S., Eds.) pp 1−17, Academic Press, New York.
9. Gilbert, W. (1986) The RNA world, *Nature 319*, 618.
10. Huang, F., Bugg, C. W., and Yarus, M. (2000) RNA-catalyzed CoA, NAD, and FAD synthesis from phosphopantetheine, NMN, and FMN, *Biochemistry 39*, 15548−15555.
11. Miller, S. L., and Schlesinger, G. (1993) Prebiotic syntheses of vitamin coenzymes: II. Pantoic acid, pantethenic acid, and composition of coenzyme A, *J. Mol. Evol. 36*, 308−314.
12. Keefe, A. D., Newton, G. L., and Miller, S. L. (1995) A possible prebiotic synthesis of pantetheine, a precursor to coenzyme A, *Nature 373*, 683−685.
13. Coleman, T. M., and Huang, F. (2002) RNA-catalyzed thioester synthesis, *Chem. Biol. 9*, 1227−1236.
14. Porta, H., and Lizardi, P. M. (1995) An allosteric hammerhead ribozyme, *Biotechnology 13*, 161−164.
15. Kuwabara, T., Warashina, M., Tanabe, T., Tani, K., Asano, S., and Taira, K. (1998) A novel allosterically trans-activated ribozyme, the maxizyme, with exceptional specificity *in vitro* and *in vivo*, *Mol. Cell 2*, 617−627.
16. Marshall, K. A., and Ellington, A. D. (1999) Training ribozymes to switch, *Nat. Struct. Biol. 6*, 992−994.
17. Soukup, G. A., and Breaker, R. R. (1999) Engineering precision RNA molecular switches, *Proc. Natl. Acad. Sci. U.S.A. 96*, 3584−3589.
18. Soukup, G. A., and Breaker, R. R. (2000) Allosteric nucleic acid catalysts, *Curr. Opin. Struct. Biol. 10*, 318−325.
19. Warashina, M., Kuwabara, T., and Taira, K. (2000) Working at the cutting edge: The creation of allosteric ribozymes, *Struct. Fold. Des. 8*, R207−R212.
20. Piganeau, N., Thuillier, V., and Famulok, M. (2001) *In vitro* selection of allosteric ribozymes: Theory and experimental validation, *J. Mol. Biol. 312*, 1177−1190.
21. Burke, D. H., Ozerova, N. D., and Nilsen-Hamilton, M. (2002) Allosteric hammerhead ribozyme TRAPs, *Biochemistry 41*, 6588−6594.
22. Kertsburg, A., and Soukup, G. A. (2002) A versatile communication module for controlling RNA folding and catalysis, *Nucleic Acids Res. 30*, 4599−4606.
23. Wang, D. Y., Lai, B. H., and Sen, D. (2002) A general strategy for effector-mediated control of RNA-cleaving ribozymes and DNA enzymes, *J. Mol. Biol. 318*, 33−43.
24. Ferguson, A., Boomer, R. M., Kurz, M., Keene, S. C., Diener, J. L., Keefe, A. D., Wilson, C., and Cload, S. T. (2004) A novel strategy for selection of allosteric ribozymes yields RiboReporter sensors for caffeine and aspartame, *Nucleic Acids Res. 32*, 1756−1766.
25. Roth, A., and Breaker, R. R. (2004) Selection *in vitro* of allosteric ribozymes, *Methods Mol. Biol. 252*, 145−164.
26. Berg, P. (1958) The chemical synthesis of amino acyl adenylates, *J. Biol. Chem. 233*, 608−611.
27. Ciesiolka, J., Illangasekare, M., Majerfeld, I., Nickles, T., Welch, M., Yarus, M., and Zinnen, S. (1996) Affinity selection-amplification from randomized ribooligonucleotide pools, *Methods Enzymol. 267*, 315−335.
28. Lorsch, J. R., Bartel, D. P., and Szostak, J. W. (1995) Reverse transcriptase reads through a 2′-5′ linkage and a 2′-thiophosphate in a template, *Nucleic Acids Res. 23*, 2811−2814.
29. Sarin, P. S., and Zamecnik, P. C. (1964) On the stability of aminoacyl-*s*-RNA to nucleophilic catalysis, *Biochim. Biophys. Acta 91*, 653−655.
30. Schuber, F., and Pinck, M. (1974) On the chemical reactivity of aminoacyl-tRNA ester bond. I. Influence of pH and nature of the acyl group on the rate of hydrolysis, *Biochemie 56*, 383−390.
31. Illangasekare, M., and Yarus, M. (1997) Small-molecule−substrate interactions with a self-aminoacylating ribozyme, *J. Mol. Biol. 268*, 631−639.
32. Zuker, M. (2003) Mfold web server for nucleic acid folding and hybridization prediction, *Nucleic Acids Res. 31*, 3406−3415.
33. Bartel, D. P., and Szostak, J. W. (1993) Isolation of new ribozymes from a large pool of random sequences, *Science 261*, 1411−1418.
34. Lorsch, J. R., and Szostak, J. W. (1994) *In vitro* evolution of new ribozymes with polynucleotide kinase activity, *Nature 371*, 31−36.
35. Lohse, P. A., and Szostak, J. W. (1996) Ribozyme-catalysed amino acid transfer reactions, *Nature 381*, 442−444.
36. Suga, H., Lohse, P. A., and Szostak, J. W. (1998) Structural and kinetic characterization of an acyl transferase ribozyme, *J. Am. Chem. Soc. 120*, 1151−1156.
37. Saito, H., Kourouklis, D., and Suga, H. (2001) An *in vitro* evolved precursor tRNA with aminoacylation activity, *EMBO J. 20*, 1797−1806.
38. Sanger, F., Nicklen, S., and Coulson, A. R. (1977) DNA sequencing with chain-terminating inhibitors, *Proc. Natl. Acad. Sci. U.S.A. 74*, 5463−5467.
39. Piccirilli, J. A., McConnell, T. S., Zaug, A. J., Noller, H. F., and Cech, T. R. (1992) Aminoacyl esterase activity of the Tetrahymena ribozyme, *Science 256*, 1420−1424.
40. Schimmel, P., Giege, R., Moras, D., and Yokoyama, S. (1993) An operational RNA code for amino acids and possible relationship to genetic code, *Proc. Natl. Acad. Sci. U.S.A. 90*, 8763−8768.
41. Illangasekare, M., Sanchez, G., Nickles, T., and Yarus, M. (1995) Aminoacyl-RNA synthesis catalyzed by an RNA, *Science 267*, 643−647.

42. Ribas de Pouplana, L., Turner, R. J., Steer, B. A., and Schimmel, P. (1998) Genetic code origins: tRNAs older than their synthetases? *Proc. Natl. Acad. Sci. U.S.A. 95*, 11295−11300.
43. Illangasekare, M., and Yarus, M. (1999) Specific, rapid synthesis of Phe-RNA by RNA, *Proc. Natl. Acad. Sci. U.S.A. 96*, 5470−5475.
44. Illangasekare, M., Kovalchuke, O., and Yarus, M. (1997) Essential structures of a self-aminoacylating RNA, *J. Mol. Biol. 274*, 519−529.
45. Illangasekare, M., and Yarus, M. (1999) A tiny RNA that catalyzes both aminoacyl-RNA and peptidyl-RNA synthesis, *RNA 5*, 1482−1489.
46. Jenne, A., and Famulok, M. (1998) A novel ribozyme with ester transferase activity, *Chem. Biol. 5*, 23−34.
47. Lee, N., Bessho, Y., Wei, K., Szostak, J. W., and Suga, H. (2000) Ribozyme-catalyzed tRNA aminoacylation, *Nat. Struct. Biol. 7*, 28−33.
48. Ramaswamy, K., Wei, K., and Suga, H. (2002) Minihelix-loop RNAs: Minimal structures for aminoacylation catalysts, *Nucleic Acids Res. 30*, 2162−2171.
49. Saito, H., and Suga, H. (2001) A ribozyme exclusively aminoacylates the 3′-hydroxyl group of the tRNA terminal adenosine, *J. Am. Chem. Soc. 123*, 7178−7179.
50. Murakami, H., Saito, H., and Suga, H. (2003) A versatile tRNA aminoacylation catalyst based on RNA, *Chem. Biol. 10*, 655−662.
51. de Duve, C. (1991) *Blueprint for a Cell: The Nature and Origin of Life*, Neil Patterson Publishers, Burlington, NC.
52. Lacey, J., Jr., Senaratne, N., and Mullins, D. W., Jr. (1984) Hydrolytic properties of phenyalanyl- and *N*-acetylphenylalanyl adenylate anhydrides, *Origins Life 15*, 45−54.
53. Jakubowski, H. (1998) Aminoacylation of coenzyme A and pantetheine by aminoacyl-tRNA synthetases: Possible link between noncoded and coded peptide synthesis, *Biochemistry 37*, 5147−5153.
54. Jakubowski, H. (2000) Amino acid selectivity in the aminoacylation of coenzyme A and RNA minihelices by aminoacyl-tRNA synthetases, *J. Biol. Chem. 275*, 34845−34848.
55. Jakubowski, H., and Fersht, A. R. (1981) Alternative pathways for editing non-cognate amino acids by aminoacyl-tRNA synthetases, *Nucleic Acids Res. 9*, 3105−3117.
56. Jakubowski, H. (1997) Aminoacyl thioester chemistry of class II aminoacyl-tRNA synthetases, *Biochemistry 36*, 11077−11085.

BI047576B